INTRUSIVE EFFECT ON GAS LIQUID FLOW MEASUREMENT BY WIRE MESH TOMOGRAPHY.

Wangjiraniran,W*., Motegi, Y., Kikura, H., Aritomi, M.[1)] Richter, S.[2)] and Yamamoto, K.[3)]

[1)] Research Laboratory for Nuclear Reactors, Tokyo Institute of Technology, 2-12-1, Ohokayama, Meguro-ku, 152-8550, Tokyo, Japan.
Tel: +81-3-5734-3063/ FAX: +81-3-5734-2959
e-mail: weerin_w@2phase.nr.titech.ac.jp

[2)] Air Liquid Japan, Ltd., 9-1 Shinonome 1-chome, Koto-ku, 135-0062 Tokyo, Japan.
Tel: +81-3-3536-2314/ FAX: +81 -3-3536-2307

[3)] The Japan Atomic Power Company, 1-1, Kandamitoshiro-cho, Chiyoda-ku, 101-0053, Tokyo, Japan.

1 Introduction

To study the characteristic of multiphase flow, various measurement techniques are applied. One of the powerful techniques is the Wire Mesh Tomography technique (WMT) developed and commercialized by FZR[1] and Teletronic[2]. The measurement is based on the dependency of void fraction on the electrical conductivity. Local properties with planar measurement can be obtained from the crossing wire between transmitter and receiver. Due to being intrusive technique, the influence of the wire sensor on the measurement and on the flow characteristic has to be carefully considered.

The disturbance level is mainly depended on the sensor configuration such as wire diameter, material, spatial resolution, etc. These properties are related to the additional external force - drag and surface tension, including the turbulent generation by viscous force. Furthermore, the force balance with the difference of flow pattern, void size and velocity is not identical and these properties are expected to change with the wire existing. For this reason, the intrusive effect study with various flow conditions is also necessary. To find out the disturbance level and its mechanism, various methods were applied in the past. Prasser et al. [1] compared the visualization between WMT and high speed video camera by transforming the signal between cross-section and Eulerian side view. The results show that the sensor causes a significant bubble fragmentation. However, the two-phase flow structure was captured before it was disturbed by the sensor. Richter et al. [2] applied the statistical methods emphasized on the repeatability of a void fraction signal from two adjacent measuring planes. The deviation from the theoretical maximum void fraction as well as the deceleration of bubbles in term of normalized void fraction gradients was presented.

---

[1] Research Center of Rossendorf, Institute for Safety Analysis, Postfach 51 01 19, 01314 Dresden, Germany.

[2] Teletronic Rossendorf of GmbH, Bautzner Landstr. 45, 01454 Grosserkmannsdorf, Germany.

In the present, the additional information of the intrusive effect on the gas-liquid flow and on the measurement with WMT is presented. The deviation of signal from two adjacent measuring planes is repeatedly focused with the varied flow pattern from bubbly to bubble-slug transition. Furthermore, the experimental method for evaluation of bubble deceleration is proposed.

2 Wire mesh tomography

The applied electrode mesh sensor is illustrated in fig 1 consisting of 3 electrode wire planes with separated 2 mm. The upper and lower planes work as the transmitter planes. Each transmitter plane consists of 8 electrodes. The middle one works as the receiver plane which consists of 32 electrodes aligning with 90 degree comparing to the transmitter. This configuration corresponds to two measuring planes (2×8×32) with the spatial resolution 2.22×3.03 mm^2. The wire diameter is 0.125 mm.

The utilized data acquisition unit is the second generation of commercial distribution with a maximum overall sampling frequency of 10 kHz. The maximum capacity is 170,000 frames. The entire signal acquisition procedure is operated and controlled by a Digital Signal Processor (DSP). The obtained data is stored in buffer memory of the acquisition unit and transferred to PC by an Ethernet interface.

3 Experimental setup

The measurement is conducted on the 20x100 mm^2 rectangular channel with total length of 1.8 m ($55D_h$) as shown in fig 2. The bubble is generated by injecting air through the steel needles. The air flow rate is measured upstream of the air injection needles by a Laminar Flow Meter (LFM) with an accuracy of 1.5%. The water flow rate is measured by the orifice with an accuracy of 2.5%. The sensor is located at 1 m downstream from the needles.

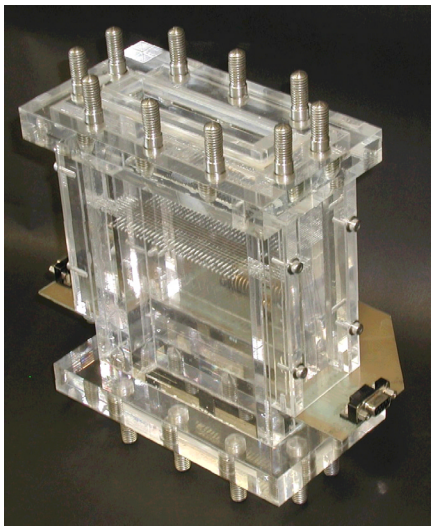

Fig.1 Wire mesh sensor

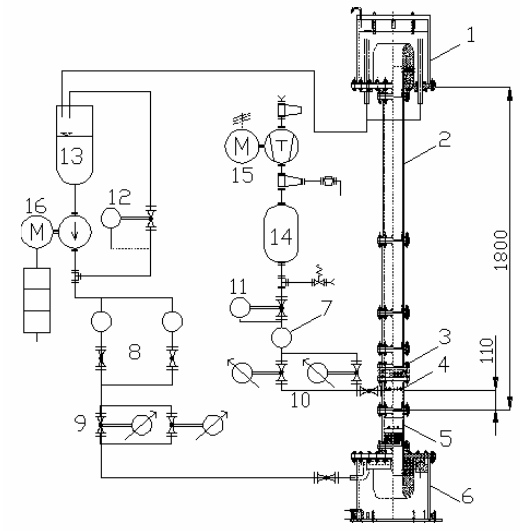

Fig.2 Experimental setup

4 Influence on the time dependent void fraction

The results with the variation of flow condition are illustrated in fig 3. The continuous air injecting of $<U_G>$=2.5, 20 and 50 mm/s with constant $<U_L>$=150 mm/s is selected and shown in fig 3a-3c. These conditions correspond to small bubble (order of sensor spatial resolution), intermediate bubble (2-5 times of sensor spatial resolution) and bubble-slug transition respectively. The imaginary time (t*) is interpreted as the downstream distance scaled from the cross-sectional averaged true gas velocity similar to Prasser et al [3]. The true gas velocity can be calculated directly with two adjacent measuring planes sensor from delay time evaluation method proposed by Richter et al [2]. For the ideal case of no wire disturbance, with a small gap between each plane, the contour shapes from both planes are expected to be identity and overlapped due to their velocity.

The contour results show the maximum reduction and more lateral spreading for the downstream plane in all condition but not for large void structure particularly in fig 3c. It can be explained by the water bridge behind the middle wire plane. The gas structure has been blocked and the volume behind the wire can not be occupied. However, the coalescent is sometime occurred when the gas structure is large enough and the maximum reduction is not observed. For line-contour with constant threshold (ε_{th}), the disappeared small bubble and unrealistic fragments are still remained. However, in this case, the comparing of the equal level is interested. The results show the interfacial deformation which is not related to the flow pattern or void size.

In addition, the result of a single slug is illustrated in fig 3d. The original shape is observed as a bullet-like shape. The result shows the interfacial deformation by the first and the middle wire plane aligned in x_2 and x_1 direction respectively. Some pocket of water phase is observed inside the air slug following the wire direction due to the water bridge behind the wire. However, from the High Speed Camera (HSC), the slug is recombined by coalescence and the original bullet shape is completely restored after the wire.

5 Influence on the averaged void fraction

The void fraction deviation between up and downstream measuring plane is illustrated in fig 4. Notice that the deviation of each measuring plane can be interpreted as the effect of the middle wire plane placed between each measuring plane. The results show that the averaged void fraction from the upstream plane is smaller than the downstream for low $<U_G>$ (less than 10 mm/s) while it is opposite for the high $<U_G>$ (larger than 10 mm/s). The minimum deviation can be observed at $<U_G>$ approximately 10 mm/s.

The deviation can be considered from the effect of deceleration and deformation of the gas structure due to the wire. When bubbles are decelerated, the duration of bubble occupied the measuring volume would be increased. This can be the reason for larger void fraction for the downstream plane and supposed to be the dominated effect in the low $<U_G>$ range. On the other hand, the deformation effect including the water bridges and fragmentation has a tendency to reduce the void fraction of the downstream plane particularly for the larger bubble size. Thus, the deformation can be considered to be the dominated effect in the high $<U_G>$ range.

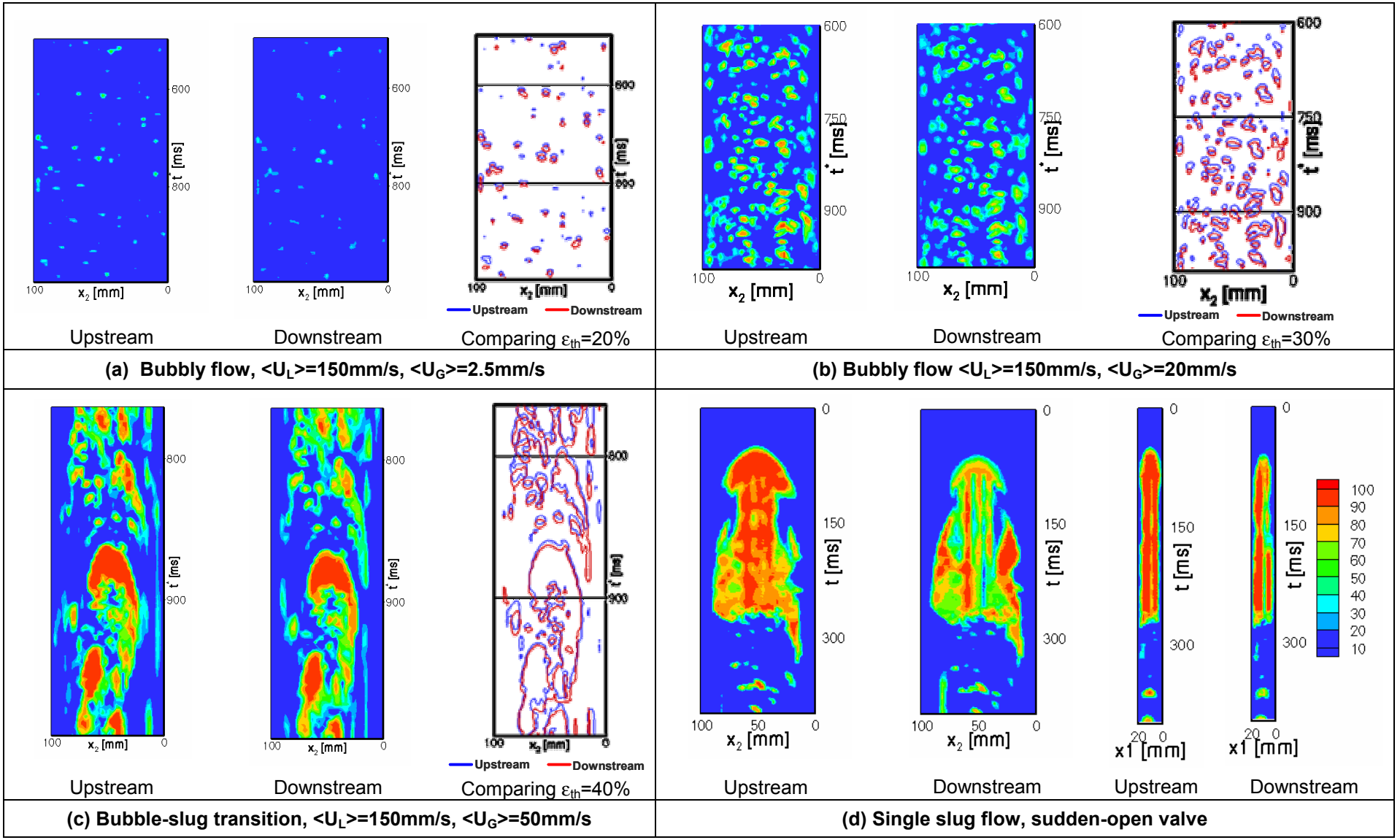

Fig 3 Comparison of the signal from two measuring planes

When further increasing <U_G> more than 10 mm/s, the deviation is obviously increased. It is due to the increasing of large scale lateral motion in the transition to slug flow regime, although large bubble can be minimized the intrusive effect in term of length scale and coalescence. Furthermore, the dependency on the <U_L> is also observed. With higher <U_L>, the deviation is minimized by decreasing the lateral mobility of the bubble similar to Richter [4].

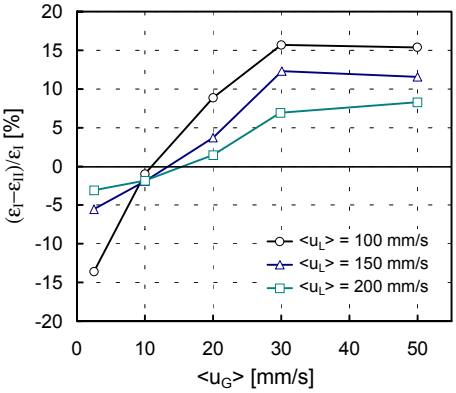

Fig 4 Void fraction deviation between up and downstream measuring plane.

The example of void fraction distribution normalized with the cross-sectional averaged value is illustrated in fig 5. From the results, the downstream data (the 2nd plane) obviously approaches the cross-sectional averaged value and significantly more uniform than the upstream (the 1st plane) particularly at <U_L> = 10 and 50 mm/s in fig 5b and 5c. To indicate the non-uniformity level, the non-uniformity coefficient, C_n, is expressed in term of the deviation from the cross-sectional averaged value according to

$$C_n = (mn)^{-1} \sum_{i=0}^{n} \sum_{j=0}^{m} \left| \overline{\varepsilon_{i,j}} - \langle \overline{\varepsilon} \rangle \right| \Big/ \langle \bar{\varepsilon} \rangle \qquad (1)$$

The variation of non-uniformity with the variation of flow condition is shown in fig 6. The non-uniformity level of the downstream plane is reduced from the upstream plane about 5-15% of the averaged value depending on the flow condition. However, the relationship between the non-uniformity reduction and flow condition can not be identified. The increasing of uniformity from the upstream plane can be explained by the nature of water bridges and fragmentation. Both phenomena have a tendency to make void structure spreading in lateral direction. This result is lead to applying the series of wire to generate the bubble uniformity particularly on the laboratory scale. For this purpose, the existing of the uniformity on the downstream of the wire has to be considered.

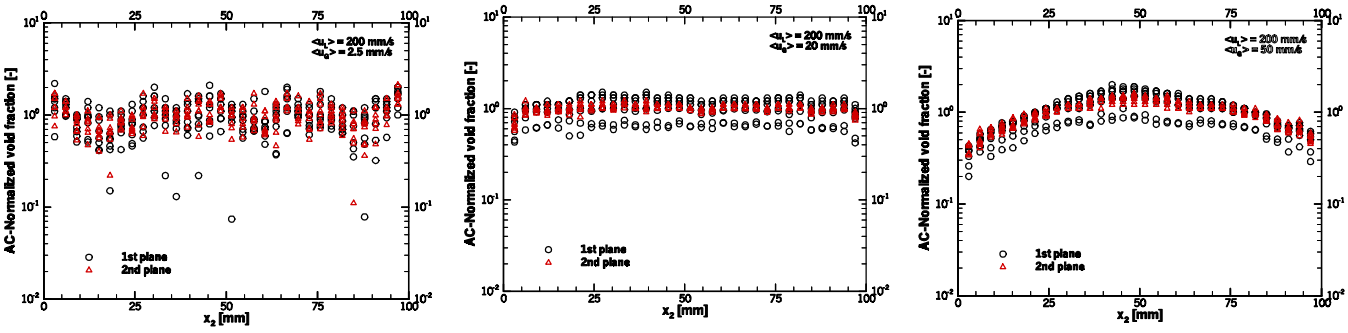

Fig 5 Normalized void fraction profile

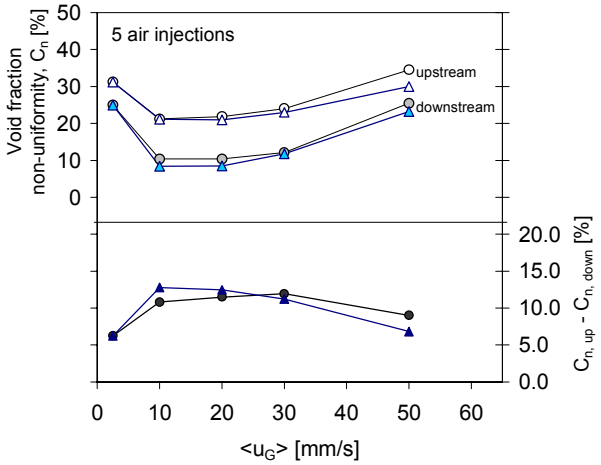

Fig 6 Void fraction non-uniformity, Cn; triangular symbol for $<U_L>$ = 100 mm/s, circle symbol for $<U_L>$ = 200 mm/s

6 Bubble deceleration

The high speed CCD camera (FastCam-Net 500/1000/Max, equipped with a standard NIKON 100 mm) is utilized. The sample of the sequence picture is shown in fig 7. The rising gas velocity is evaluated from the duration which bubble surface migrated within the specified axial length, in this case, equal to the distance of adjacent plane. The rising gas velocity of each void structure is estimated from the averaged velocity of the frontal and the trailing surface. The Eulerian frame is statically located at the middle half of the channel. Due to the visualization limit at high gas intensities, the experiment is carried out at only low void fraction, in this case, constant $<U_G>$ = 1 mm/s and $<U_L>$ = 0-200 mm/s corresponding to the upstream bubble rising velocity about 200-400 mm/s.

The results of the evaluated frontal and trailing surface velocity are illustrated in fig 8. For upstream of the sensor, there is no significant difference between frontal and trailing surface velocity within the uncertainty. Within the sensor, the frontal surfaces are slightly faster than the trailing surfaces. The significant deformation within the sensor comparing to the upstream flow is observed. Notice that the frontal surfaces velocity at this position can be understood as the average velocity during the deceleration while the trailing surface velocity is the averaged recovery velocity when it accelerates. The slightly faster velocity of the frontal surface can be proposed by the inertial effect of the upstream flow. At slightly downstream from the sensor ($x\sim2\delta$), oppositely, the frontal surface migrates slower than the trailing surface. At this position, the frontal velocity is evaluated with wire existing while the rare velocity is not. At further downstream ($x\sim4\text{-}8\delta$), the difference between both surface is disappeared and supposed to be not effect by the wire.

The results of the averaged and normalized surface velocity are illustrated in fig 9a and 9b. The results show that the characteristic of the bubble slow down is similar in this flow condition range. The velocity is decreased almost 50% of the upstream value within the wire region. Furthermore, the sensor does not affect to upstream flow within the spatial resolution (2δ) while it affect to $4\text{-}8\delta$ of the downstream flow.

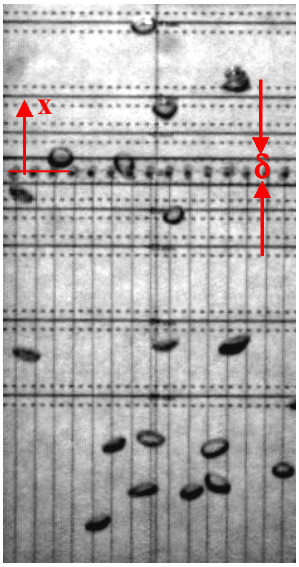

Fig 7 Example of picture frame from high speed video camera

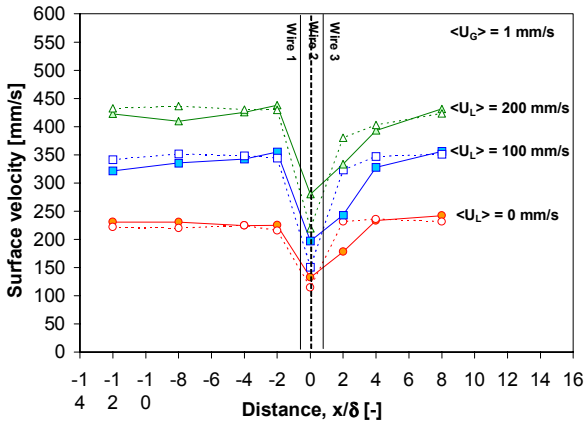

Fig 8 Surface velocity distribution; full line: front surface, dot line: rare surface

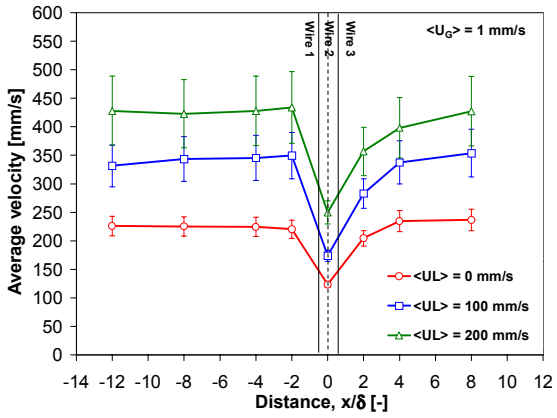

(a) Evaluated value

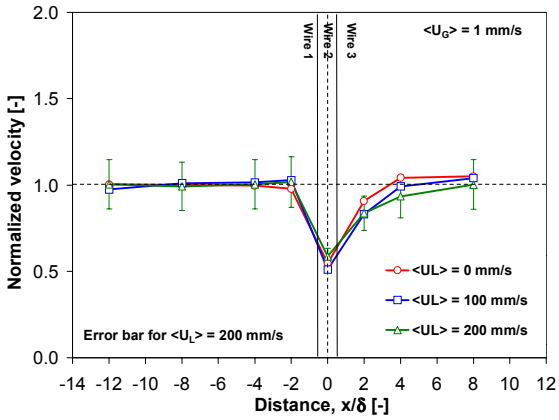

(b) Normalized with the upstream value

Fig 9 Averaged surface velocity distribution

7 Conclusions

1) The contribution of deceleration and deformation on the intrusive effect with varied flow condition is proposed. The minimized condition is observed at $\langle U_G \rangle$ about 10 mm/s. In addition, the reduction of lateral motion by increasing of $\langle U_L \rangle$ is confirmed.
2) The void fraction uniformity of downstream plane is increased from the upstream plane due to the wire with 5-15% depending on the flow condition.
3) The slow down characteristics is similar in this flow condition range. The velocity is decreased almost 50% of the upstream value within the wire region. Furthermore, the sensor does not affect to upstream flow within the spatial resolution (2δ) while it affect to 4-8δ of the downstream flow.

8 Nomenclature

sign	unit	denomination
<>	index	Cross-sectional average
-	index	Time average
δ	mm	Axial length scale of the sensor (3mm)
ε_I	1	Void fraction obtained from the upstream measuring plane
ε_{II}	1	Void fraction obtained from the downstream measuring plane
ε_{th}	1	Void fraction threshold level
U_G	mm/s	Superficial gas velocity
U_L	mm/s	Superficial water velocity

9 References

[1] Prasser, H.-M., Scholz, D., Zippe, C., Bubble Size Measurement using Wire-mesh Sensor, Flow measurement and Instrumentation, 12 (2001), 299-312.

[2] Richter, S., Aritomi, M., Prasser, H.-M., Hampel, R., Approach Towards Spatial Phase Reconstruction in Transient Bubbly Flow using a Wire-mesh Sensor, International Journal of Heat and Mass Transfer, 45 (2002), 1063-1075.

[3] Prasser, H-M., Zshau, J., Peters, D., Pietzsch, G., Taubert, W., and Trepte, M., Fast Wire-mesh Sensors for Gas-liquid Flows-visualization with upto 10,000 frames per second, International Congress on Advance Nuclear Power Planes, June 9-13, Hollywood Florida, USA.